PAPER

CrossMark
← click for updates

Self-assembly of a cholesteryl-modified nucleoside into tubular structures from giant unilamellar vesicles†

Luisa Losensky,[a] Salvatore Chiantia,[a] Gudrun Holland,[b] Michael Laue,[b] Anca Petran,[c] Jürgen Liebscher[c] and Anna Arbuzova*[a]

We recently reported the formation of micro- and nanometer thick tubules in a binary system of cholesteryl-modified aminouridine and a phosphatidylcholine in aqueous solution upon cooling from 70 °C to room temperature (Pescador *et al.*, *Chem. Commun*, 2010, **46**, 5358). To better understand the first steps of the tubular self-assembly and the role of the phospholipid, we investigated now morphological changes of phosphatidylcholine giant unilamellar vesicles upon incorporation of the conjugate at room temperature. We observed formation of needle-like structures organized in rosettes or bundles within hours to days depending on the mole fraction of the conjugate and preparation technique. Transmission electron microscopy revealed that the needle-like structures were 100–200 nm thick tubules with the inner lumen diameters of 15–40 nm. The tube self-assembly occurred at room temperature, which is important for further development of biomedical applications.

Introduction

Self-assembly of amphiphilic molecules into micelles, vesicles, sheets, or tubular structures are governed by an interplay of hydrophobic interactions, hydrogen bonding, stacking, structure (form, chirality) of the molecules, and interaction with the solvent.[1–5] The pseudo one-dimensional needle-like and tubular structures are of particular interest, as they are not only found in nature, *e.g.* cholesterol (Chol) needle-like crystals in bile and atherosclerotic plaques,[6,7] but can be also used for different applications, *e.g.* as templates for inorganic nanotubes and wires, drug-delivery systems, single-molecule sensing, cleaning of water,[8–10] and for structuring of edible oils to margarine.[11]

Different mechanisms were suggested for the formation of the tubular structures: rolling of membrane sheets, fusion of vesicles, growth of helical structures in width or decreasing pitch.[12,13] However, the mechanism of the tubular structure assembly is still not well understood; especially as different assembly mechanisms were found in binary systems depending on the molar ratio of the components.[14]

Both cholesterol and nucleoside derivatives were reported to self-assemble into needles, helices, tubular structures, or

vesicles.[10,15,16] Sharp needle-like crystals, micrometer-sized helices, and tubules mostly made of cholesterol were found in both patient samples and model bile mixtures.[6,17,18] A native bile salt component, sodium lithocholate, was found to form single molecular layer tubes with diameters about 50 nm.[19] Lithocholic acid formed tubules in aqueous solution of pH 12 with a continuous growth of the tubules as long as vesicles were present.[20] Chemically modified bile salts, *e.g.* a sodium cholate derivative, self-assembled into tubules of about 450 nm diameter and length up to 7 μm when heated above 40 °C.[21,22] Uracil-modified cholesterol was reported to form fibers/columnar structures in organic solvents. However, only precipitation was observed in aqueous solutions.[23] Other cholesteryl conjugates of nucleosides, *e.g.* acyclovir and zidovudine commonly used as antiviral drugs, formed 100–200 nm size bilayer vesicles in aqueous solutions when injected from THF.[24]

We have reported on the micro- and nano-tubule formation from 2′-*N*-(2-(cholesteryl)-succinyl)-2′-deoxy-2′-aminouridine (CholAU, Fig. 1A) with 1,2-dioleoyl-*sn*-glycero-3-phosphocholine (DOPC) upon cooling of a 30 : 70 CholAU : DOPC (mol%) aqueous suspension from 70 °C to room temperature.[25] CholAU combines self-assembly properties of cholesterol (hydrophobicity, chirality) and uridine (stacking, hydrogen bonding). To understand the first steps of the tubular self-assembly and the role of the phospholipid, we now investigated morphological changes of phosphatidylcholine (PC) and CholAU binary system upon the incorporation of CholAU into PC giant unilamellar vesicles (GUVs) using several approaches: (i) from a complex with methyl-β-cyclodextrin (mβCD–CholAU) to assure incorporation of monomeric CholAU into the lipid membrane; (ii) from DMSO

[a]Humboldt-Universität zu Berlin, Institut für Biologie, Invalidenstr. 42, 10115 Berlin, Germany. E-mail: arbuzova@cms.hu-berlin.de

[b]Robert Koch Institute, ZBS 4, Nordufer 20, 13353 Berlin, Germany

[c]National Institute of Research and Development for Isotopic and Molecular Technologies, Donath 65-103, RO-400293 Cluj-Napoca, Romania

† Electronic supplementary information (ESI) available. See DOI: 10.1039/c4ra11289j
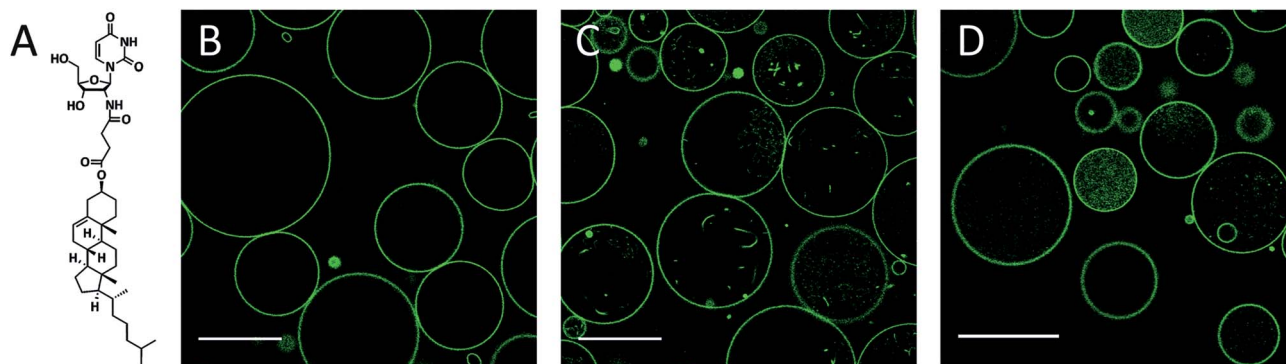
Fig. 1 (a) Chemical structure of the conjugate 2′-N-(2-(cholesteryl)-succinyl)-2′-deoxy-2′-aminouridine (CholAU). (b–d) NBD fluorescence images: DMoPC : NBD-DMPE 99.2 : 0.8 (molar ratio) GUVs at times 0 s and 30 min after exchange of 5 mM glucose with 2.5 mM mβCD–CholAU solution (b) and (c), respectively. (d) GUVs 30 min after exchange of the solution to 5 mM mβCD. Scale bars correspond to 50 μm.

solution of CholAU; and (iii) by preparation of GUVs starting with a CholAU–PC mixture in organic solvent for a better control of the incorporated amount.

GUVs are widely used models of cell membranes and consist of unilamellar vesicles with typical dimensions in the μm-range. Their size and curvature resemble those of actual cellular plasma membranes and, moreover, are compatible with the application of optical microscopy.[26,27] GUVs have been successfully used in the last years to investigate lipid–protein interactions, membrane protein lateral organization,[28] membrane curvature and tubule formation,[29–31] lipid–lipid interaction, e.g. PC–Chol interaction,[32–34] and specific domain partitioning of lipid-modified conjugates.[35–37]

The self-assembly of the tubular structures from GUVs containing CholAU was investigated by fluorescence and electron microscopy. The results provide information on the role of phospholipid vesicles in the tubular self-assembly and in how far the uridine moiety of CholAU changes the interaction with lipid membranes in comparison with published results obtained with cholesterol.

Experimental

Chemicals

1,2-Dimyristoleoyl-sn-glycero-3-phosphocholine (DMoPC) and 1,2-dimyristoyl-sn-glycero-3-phosphoethanolamine-N-(7-nitro-2-1,3-benzoxadiazol-4-yl) (ammonium salt), (NBD-DMPE) were purchased from Avanti Polar Lipids (Alabaster, AL). Methyl-β-cyclodextrin (mβCD, 1.6–2.0 mol CH_3 per unit anhydroglucose) and sucrose were purchased from Sigma-Aldrich (Taufkirchen, Germany). Chloroform and methanol were supplied from Merck (Darmstadt, Germany). Glucose was obtained from Roth (Karlsruhe, Deutschland) and 2′-N-(2-(cholesteryl)-succinyl)-2′-desoxy-2′-aminouridine (CholAU) was synthesized as described previously.[25]

Giant unilamellar vesicles

Giant unilamellar vesicles (GUVs), 30 nmol total lipid, were formed from 99.2 : 0.8 DMoPC : NBD-DMPE (molar ratio) by electroformation[38] in 5 mM sucrose solution using homemade flow chambers with an observation volume of about 300 μL as described previously.[39] For fluorescence microscopy, GUVs remained attached to the indium tin oxide (ITO) coated slides allowing efficient exchange of the solvent. For electron microscopy, GUVs were grown on platinum wires in 300 mOsm sucrose solution in homemade chambers. Upon formation, they were collected and carefully pipetted into a 300 mOsm glucose solution. For the preparation of the DMoPC : CholAU : NBD-DMPE mixtures in chloroform–methanol as solvent, the total lipid amount was kept at 30 nmol, using 40, 20 and 10 mol% CholAU (molar ratios: 59.2 : 40 : 0.8, 79.2 : 20 : 0.8 and 89.2 : 10 : 0.8 of DMoPC : CholAU : NBD-DMPE).

Preparation of mβCD–CholAU complex

Methyl-β-cyclodextrin (mβCD) and CholAU were mixed shortly before addition to DMoPC GUVs or overnight. For the shortly mixed complex, 0.8 μmol of CholAU were dissolved in $CHCl_3$–MeOH (5 : 1) in glass vials and dried using nitrogen gas. The CholAU-film was dispersed in 100 μL of 25 mM aqueous solution of mβCD, shortly sonicated and incubated in a shaker for 30 min at room temperature. For the overnight mixed complex, 0.8 μmol of CholAU and 2.5 μmol of mβCD were dissolved in 150 μL MeOH, vortexed at room temperature, dried using nitrogen stream and kept at high vacuum for 1 h. After dispersing in 150 μL ddH₂O, the solution was sonicated for 3 min and incubated in a shaker at 37 °C overnight.[40] The solution in the GUV chambers was exchanged to a 2.5 mM solution of mβCD–CholAU (calculated molar ratio 3 : 1) by injecting 600 μL through the chamber. As a control experiment the influence of mβCD on GUVs was tested. For this, 600 μL of 5 mM mβCD were injected into the chamber. The assembly process of needle-like structures was qualitatively similar independently of the duration of the mβCD–CholAU mixing step.

Addition of CholAU in DMSO

20 μL of 1 mg mL⁻¹ CholAU solution in DMSO were mixed with 580 μL water, yielding a final CholAU concentration of 47 μM. This solution was immediately injected into the flow chamber

containing 100 μM DMoPC : NBD-DMPE GUVs (*i.e.* 30 nmol in the 300 μL chambers, see above). Incorporation of all CholAU into GUVs would correspond to ~30 mol% of CholAU of total lipid.

Confocal microscopy

Olympus Fluoview FV-1000MPE, Inverted Laser Scanning microscope, Olympus (Tokyo, Japan) was used with a 488 nm Argon laser and 60×/1.2 Water UPlanSApo objective. Laser light was directed to a sample and separated from emitted light with a dichroic mirror (DM 405/488/559/635), NBD fluorescence was recorded between 500 and 600 nm with 4 μs/pixel exposure. Note, low level of irradiation is important, as strong irradiation induces GUVs shape changes, lipid oxidation, and domain formation.[41] Contrast of the fluorescence microscopy images was linearly enhanced.

Mass spectrometry

βCD–CholAU complexes were prepared as previously described[42] using acetonitrile instead of MeOH. The formation of complexes was shown by ESI-FTICRMS (electrospray ionization-Fourier transform ion cyclotron resonance mass spectrometry). Samples were measured on an Ionspec QFT-7, Varian Inc. (Lake Forest, CA), equipped with a 7 T super-conducting magnet and a Micromass Z-Spray ESI-Source, Waters Co. (Saint-Quentin, France). Solvent flow rate was adjusted to 4 μL min^{-1}, spray voltage was set to 3.8 kV. All other parameters were adjusted for an optimized detection of $[\beta CD–CholAU-H]^-$ and $[\beta CD_2–CholAU-2H]^{2-}$ complexes.[43]

Negative staining transmission electron microscopy (TEM)

To allow the transfer of the samples onto electron microscopy grids, DMoPC : NBD-DMPE 99.2 : 0.8 (molar ratio) GUVs were grown on platinum wires in 300 mOsm sucrose and transferred into 300 mOsm glucose solution in plastic tubes. CholAU was incubated with mβCD either 30 min or overnight as described above. 50 μL of 100 μM GUVs were added to 250 μL of 300 mOsm glucose solution. Then 50 μL of the 2.5 mM mβCD–CholAU solution were added. For negative staining TEM glucose was removed by sedimentation and resuspension with distilled water. A small volume (5 μL) of the suspension was adsorbed at Pioloform coated, carbon stabilized and alcian blue treated (Fluka, 1% in 1% acetic acid in water) copper grids. Excess suspension was removed by gently blotting with a wetted filter paper and the sample was stained with 0.25% aqueous uranyl acetate. The samples were analyzed using a TEM 902 (Zeiss, Oberkochen; Germany) operated at 80 kV. Micrographs were recorded with a slow scan CCD – camera (Proscan, Scheuring, Germany). Dimensions of 96 tubules from 4 samples were measured using ImageJ.

Results and discussion

Formation of needle-like structures upon incubation of DMoPC GUVs with mβCD–CholAU complex

DMoPC GUVs formed in 5 mM glucose by electroformation on indium tin oxide (ITO) coated slides were 10–50 μm ($n = 68$) in diameter and had almost no membrane structures inside (Fig. 1B). The glucose solution was exchanged with a 2.5 mM aqueous solution of CholAU pre-incubated with methyl-β-cyclodextrin (mβCD). Water-soluble cyclodextrins are capable of complex formation with lipids, *e.g.* mβCD was used to produce asymmetric liposomes,[39,40] to extract Chol from membranes[44] and to change Chol concentration in cells.[45] We used mβCD to solubilize CholAU and deliver it to lipid bilayers in an aqueous solution, which is important when working with pre-formed lipid membranes, *e.g.* GUVs. Mass spectrometry measurements revealed 1 : 1 and 2 : 1 ($[\beta CD–CholAU-H]^-$ and $[\beta CD_2–CholAU-2H]^{2-}$) complexes of the structurally and functionally related unmethylated βCD and CholAU.

Membrane tubules and smaller vesicles were detected in most GUVs after incubation with mβCD–CholAU for 30 min (Fig. 1C). These invaginations were probably formed due to the incorporation of CholAU first into the outer membrane of the vesicles. Vesicle shape deformations and budding/tubule formation were reported upon a local change of the membrane composition or environment.[30,31,46–49] For example, tubular invaginations of 240 nm diameter were observed upon aqueous phase separation (osmotic stress) in DOPC/ganglioside GUVs.[50] Although cholesterol was reported to flip quickly and spontaneously into the inner leaflet with a flip-flop halftime in the order of 1 min for liquid disordered membranes,[51,52] it is not known yet how fast CholAU can cross the membrane. Note after incubation of GUVs with mβCD alone, some GUVs revealed green fluorescence inside of the vesicles and occasionally budding/invaginations were also observed as shown in Fig. 1D. The mβCD does not penetrate through the membrane of the GUVs, but, occasionally, some GUVs might be temporarily leaky, potentially resulting in mβCD influx into the GUVs and extraction of the fluorescent dye. Then the GUV would reseal and the mβCD-dye complexes stay in the lumen of the vesicle, giving rise to the fluorescence inside some of the vesicles in control measurements as seen in Fig. 1D.

Although, at concentrations of mβCD below 10 mM no considerable extraction of phospholipids was reported, a variable extent of cyclodextrin–phospholipid interactions was observed in different studies.[53] Hence, for a phospholipid with short acyl chains and low lipid/mβCD ratio used, limited lipid extraction could occur also at a concentration of mβCD below 5 mM. Since DMoPC would be extracted only from the outer leaflet, the *trans*-bilayer mass misbalance might cause negative curvature, thus explaining the invagination of the bilayer that was occasionally observed in control samples.

Three hours after addition of the complex, compact optically dense fluorescent needle-like structures were observed as shown in Fig. 2A. The needle-like structures were organized in rosettes with a few vesicles in between on the glass surface,
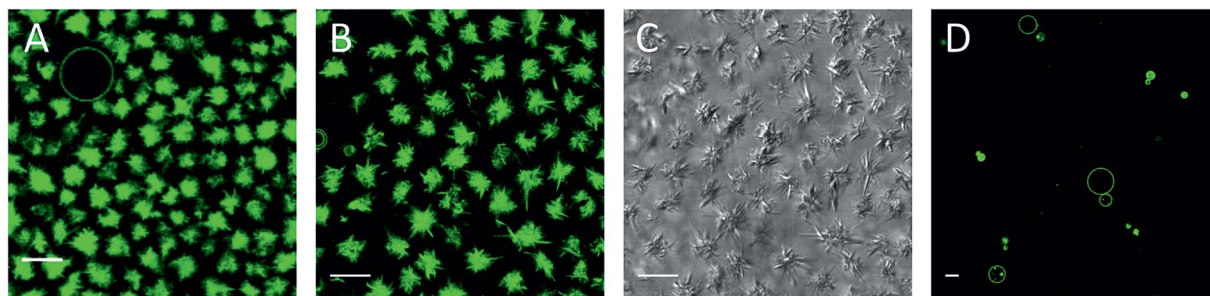
Fig. 2 Needle-like structures 3 hours (a) and one day (b and c) after addition of 2.5 mM mβCD–CholAU to DMoPC : NBD-DMPE 99.2 : 0.8 (molar ratio) GUVs. (a, b and d) NBD fluorescence, (c) differential interference contrast (DIC) images, respectively. (d) Control: GUVs one day after exchange of the solution to 5 mM mβCD. Scale bars correspond to 10 μm.

whereas above the glass surface still more vesicles were found (not shown). We assume that upon incorporation of monomeric CholAU into the PC membrane, metastable structures were formed with a tendency for a phase separation leading further to the formation of stable needle-like structures. Sometimes, single needle-like structures covered with lipid bilayer structures were observed inside of the vesicles (see Fig. 5B). Needles grew larger, causing deformation of the vesicle shape and then the vesicle ruptured. Therefore, the number of GUVs decreased in time (hours). Similar rupture of vesicles caused by lysozyme crystals growth was reported previously.[54] One day after mβCD–CholAU addition, predominantly needle-like structures with some GUVs were observed (Fig. 2B and C). 6 days after mβCD–CholAU addition, almost no GUVs were left whereas the needle-like structures were mostly found on the glass surface organized into rosettes or bundles as well as in the solution above (not shown). In the control samples containing 5 mM mβCD no needle-like structures were observed at any time (Fig. 2D, one day after solution exchange).

Addition of CholAU to GUVs from DMSO solution also led to assembly of needle-like structures

Alternatively, CholAU was solubilized in DMSO. This solvent was reported to have no or little effect on the bilayer structure and GUVs when added at low concentrations (0.16–0.5 v/v%).[55] We also observed no significant effect of DMSO addition on DMoPC GUVs (Fig. 3A); mostly unilamellar vesicles with average diameters of 10–40 μm ($n = 78$) were observed 1 hour after addition of 20 μL DMSO in 580 μL water to the flow chamber (3.3 v/v%). When a solution of 47 μM CholAU in DMSO was injected, multilamellar and aggregated vesicles were observed after 30 min as shown in Fig. 3B. If all the CholAU molecules were incorporated, this would correspond to about 30 mol% of CholAU of total lipid.

Four days after addition of CholAU as a DMSO solution, μm-long needle-like structures organized in bundles and aggregates of shorter needles were observed (Fig. 3C and D). This supports our observation that CholAU in the PC membrane was in a metastable state, which matured slowly into the stable needle-like structures.

Decreasing mole fraction of CholAU slows the rate of assembly of the needle-like structures

We further investigated the morphological changes of lipid vesicles induced by CholAU in GUVs prepared with ∼40, 20, and 10 mol% CholAU by electroformation in the flow chambers. For a 59.2 : 40 : 0.8 DMoPC : CholAU : NBD-DMPE mixture, large GUVs were not formed. Only smaller and multilamellar vesicles with diameters of about 1–10 μm, pearl necklaces (see insert in Fig. 4A), and aggregates were observed as shown in Fig. 4A. Formation of necklaces upon phase separation in DPPC : POPC : Chol vesicles containing 40 mol% of Chol were reported.[56]

For a 79.2 : 20 : 0.8 DMoPC : CholAU : NBD-DMPE mixture, large but non-round shaped GUVs were formed (Fig. 4B). Smaller and partly multilamellar vesicles were also observed. Non-round vesicle shape might indicate inhomogeneous
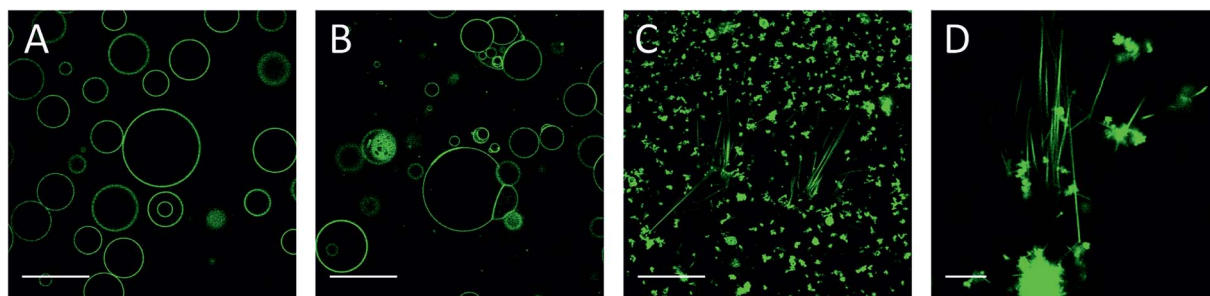

Fig. 3 (a) DMoPC : NBD-DMPE GUVs 1 hour after addition of 20 μL DMSO and 580 μL water. (b) DMoPC : NBD-DMPE GUVs 30 min after addition of 47 μM CholAU in 20 μL DMSO and 580 μL water. (c) and (d) The same sample as in (b) 4 days after addition of 47 μM CholAU in 20 μL DMSO and 580 μL water. NBD fluorescence images. Scale bars correspond to 50 μm for (a–c) and 10 μm for (d).
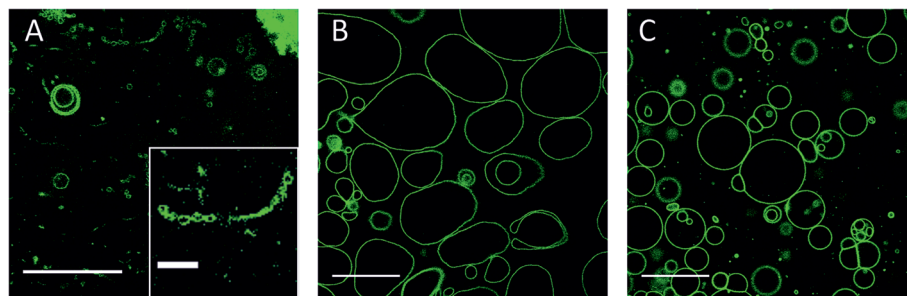
Fig. 4 Morphology of the vesicles formed by electroformation depends on the mole fraction of CholAU in the mixture. NBD fluorescence images of (a) 59.2 : 40 : 0.8, (b) 79.2 : 20 : 0.8 and (c) 89.2 : 10 : 0.8 (molar ratios) DMoPC : CholAU : NBD-DMPE samples, respectively. Scale bars correspond to 50 μm. Contrast was linearly enhanced. The insert in (a) shows a typical necklace structure observed, scale bar 10 μm.

distribution of DMoPC and CholAU in the lipid film on the ITO coated glass from which GUVs were prepared. For a 89.2 : 10 : 0.8 DMoPC : CholAU : NBD-DMPE mixture, round vesicles with diameters of about 10–40 μm ($n = 68$) and aggregates of several (3–10) vesicles as well as much smaller vesicles were observed as shown in Fig. 4C. Similarly to these results, we did not observe giant vesicles for 30 : 70 mol% CholAU : DOPC mixture upon hydration at 50 °C.[25]

Fig. 5 Needle-like structures formed at different time depending on the mole fraction of CholAU in the mixture. NBD fluorescence images: (a) one day and (b, c) 6 days after preparation of (a) 59.2 : 40 : 0.8, (b) 79.2 : 20 : 0.8 and (c) 89.2 : 10 : 0.8 (molar ratios) DMoPC : CholAU : NBD-DMPE samples, respectively. Scale bars are 50 and 10 μm for the images in the right and left panels, respectively.

One day after the preparation, μm-long needle-like structures were observed only in the 59.2 : 40 : 0.8 DMoPC:CholAU:NBD-DMPE sample (Fig. 5A). The clusters of needles were found on the glass surface and in the solution above. For lower mol% of CholAU, the rate of formation of the needle-like structures was significantly slower: six days after preparation the needle-like structures were observed in the 79.2 : 20 : 0.8 DMoPC : CholAU : NBD-DMPE sample, but not yet in the 89.2 : 10 : 0.8 DMoPC : CholAU : NBD-DMPE sample as shown in Fig. 5B and C. In the latter mixture a few needle-like structures were formed nine days after the preparation (not shown). It should be noted that in the sample with 20 mol% of CholAU, vesicle necklaces and needle-like structures covered by lipid tethers were observed even six days after preparation, indicating ongoing assembly (Fig. 5B, right). In line with this observation, non-round shaped GUVs were present in the sample with 10 mol% of CholAU six days after preparation (Fig. 5C, right panel) indicating an even earlier stage of the assembly process comparable to the vesicle shape changes upon initial incorporation into the pre-formed GUVs membrane. As discussed above, formation of the necklaces and non-round shaped vesicles might be an indication of a phase separation, which presumably occurs before the needle-like structures assemble.

We observed decreased assembly rate with decreased mol% of CholAU: the slower assembly rate might come from a slower de-mixing of CholAU and DMoPC in a membrane with less CholAU. A slow aggregation of GUVs with 10 mol% of CholAU might allow a local enrichment of CholAU in the lipid membrane upon a phase separation. A faster formation of the needle-like structures in the samples containing 30–40 mol% (hours) than 10–20 mol% (days) indicates that a solubility threshold of CholAU in DMoPC is probably around 40 mol%.

Most studies on the interaction of Chol with lipid vesicles were performed using max. 30–40 mol% Chol.[33,35,36,57–59] No crystallization was reported upon loading of DOPC GUVs with Chol up to 30–40 mol% from mβCD–Chol complex. Incorporation of up to 30 mol% cholesterol from 10–12 mM Chol–mβCD[51] into DOPC vesicles led to 40% decrease of the diffusion coefficient of a fluorescent lipid analogue indicating an increase of lipid packaging and membrane order, but no separation of optically dense structures from DOPC GUVs was observed.[33,39] The solubility limit of Chol in
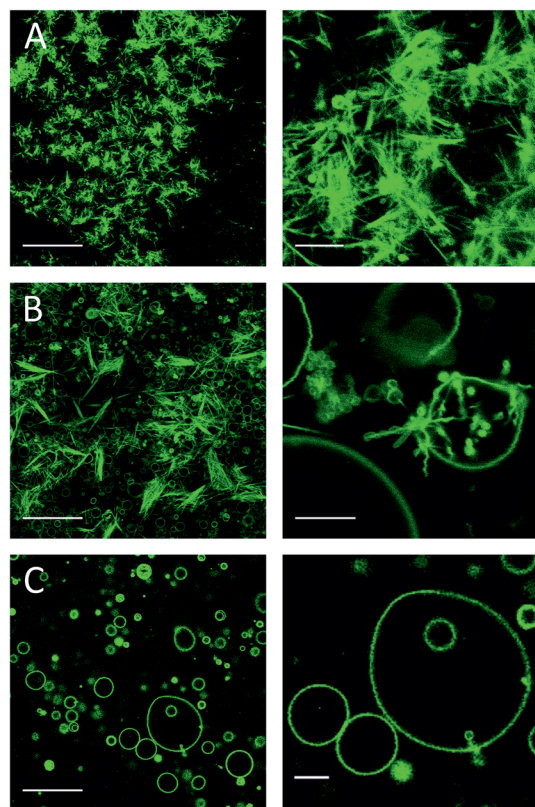
phospholipids depends on the phospholipids used; threshold of 66–67 mol% was reported for DOPC and DMPC bilayers.[60–65] We suppose that incorporation of a higher cholesterol concentration into phosphatidylcholine vesicles would lead to segregation and following precipitation of cholesterol in a form of flat and needle-like structures.

On one hand, the observation that needle-like structures formed promptly when CholAU was delivered using mβCD suggested that the accumulation of CholAU on one leaflet (*i.e.* the outer leaflet in this case) might play an important role in the assembly process. The underlying assumption here is that the flip-flop of CholAU is much slower than that of cholesterol, the latter having much smaller polar head and flip-flop halftime of seconds to 1 minute.[51,52] Accordingly, during the process of tubule formation (30–180 minutes, Fig. 1 and 2), CholAU probably did not have the time to flip and equilibrate through the bilayer. On the other hand, if CholAU was present already during GUV formation, we assumed that the molecule was more evenly distributed between the leaflets (see the low membrane curvature in Fig. 4B, $\ll 1\ \mu m^{-1}$). In this case, the process of needle formation was indeed ~100-fold slower.

Needle-like structures are tubules

We used electron microscopy to study the morphology of the needle-like structures formed. Precipitates were observed on the bottom of the tubes one day after addition of the 2.5 mM mβCD–CholAU complex to DMoPC : NBD-DMPE 99.2 : 0.8 (molar ratio) GUVs in 300 mOsm glucose solution. Fluorescence microscopy revealed rosettes of the needle structures as shown in Fig. 6A. For transmission electron microscopy (TEM), the glucose was removed by sedimentation of the needles and resuspension with water; otherwise presence of glucose might impair the visibility of structures (*e.g.* due to formation of thick and dense films due to the drying and staining process). Aggregates of flat and needle-like structures and single needle-like structures were observed in TEM (Fig. 6B and C). The aggregates resembled rosettes seen in fluorescence microscopy, however, the needles sticking out of the aggregate were significantly shorter. Presumably needles in rosettes were disturbed by the solution exchange and drying procedure. This indicates that weak interactions kept single structures organized into rosettes; this organization was presumably governed by a

phospholipid layer (hydrophobic interaction), which would be destroyed upon transfer to the rsc grids and drying. Higher magnification revealed that the needle-like structures represent tubules that withstood drying (Fig. 6C). The tubules had an average outer diameter of 100–200 nm and a length of 1–3 μm with some tubules being as long as 15 μm ($n = 96$). The inner lumen of the tubules partly filled with the contrast agent had on average diameters of 15–50 nm. Box plots of the tubules dimensions are shown in ESI.†

Differential interference contrast (DIC) images revealed optically dense needle-like structures (Fig. 2C). In TEM we observed that the structures were tubules with dense walls of 50–100 nm thickness, which explained the high contrast in DIC. The tubules withstood air drying as seen before for ~300 nm diameter CholAU–DOPC tubules formed upon cooling from 70 °C.[25] The tubules were enriched in CholAU containing up to 90 mol% of CholAU and covered by a phospholipid membrane in a fluid crystalline state.[25] Here, again homogeneous distribution of the NBD-DMPE fluorescence in the needle-like structures was observed indicating that the structures were probably covered by a phospholipid layer. Phosphatidylcholine plays multiple roles in supporting the assembly of tubules. First, the phospholipid is a solvent for CholAU preventing precipitation of the pure conjugate in aqueous solutions. Similarly, solubility of Chol in human bile depends on the PC structure and Chol–PC ratio; precipitation of Chol with transformation through helices and tubules to flat monohydrous crystals were observed for Chol super-saturated bile.[66–68] Second, lipid bilayers serve as a platform (two-dimensional phase) for the initial de-mixing of CholAU. Taking a parallel to Chol again, separation of Chol into clusters was reported for concentrations exceeding the saturation threshold.[61,65,69] Third, phospholipid vesicles changing upon formation of the intermediate aggregates, provide the necessary environment for tubular formation, which otherwise often can be seen only in organic solvents. Formation of multilamellar structures might provide the necessary environment for further self-assembly. We previously observed that CholAU–DOPC tubules were formed only inside lipid vesicles aggregates.[25] It was reported that nucleation of the cholesterol crystal growth in bile was initiated upon formation of multilamellar vesicles.[18] Fourth, the tubules are covered by a fluid layer of lipids,[25] which presumably stabilizes the tubules in the aqueous solution providing a hydrophilic surface.
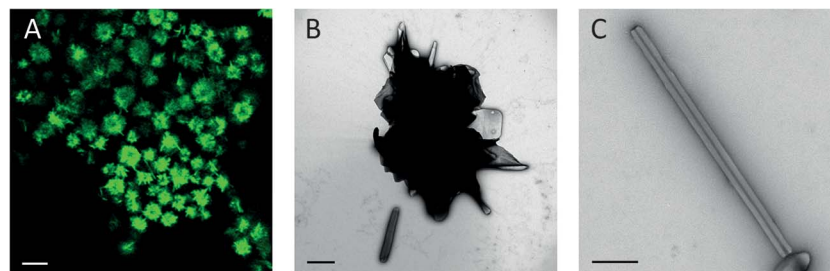

Fig. 6 (a) NBD fluorescence image of the needle-like structures organized in rosettes 20 hours after addition of 2.5 mM of mβCD–CholAU complex to DMoPC : NBD-DMPE GUVs. Scale bar corresponds to 10 μm. (b) TEM image of a rosette-like structure with tubules. (c) TEM image of a single tubule. Scale bars correspond to 1 μm and 500 nm for (b) and (c), respectively.

The self-assembled structures in the phospholipid–CholAU binary system resemble microscopically the structures reported for cholesterol self-assembly from oversaturated bile solutions. Comparing our findings to the reported for cholesterol assembly we might get further insight into the properties of the system, even though CholAU needle-like structures formed in the presence of phospholipid bilayers, whereas cholesterol assembly occurs from oversaturated mixed micelles. The needle-like structures formed from cholesterol in bile solution are thought to be anhydrous or a mixture of anhydrous and monohydrous Chol crystals covered by one layer of phosphatidylcholine.[6,59,70] Needle-like structures are considered to be a precursor for further cholesterol crystallization through helices and tubules ending with flat crystals of monohydrous Chol.[67,71] In contrast, we observed that both CholAU–PC tubules and flat crystals were stable for several months. We do not have enough evidence yet to report the state of CholAU in the structures, whereas we have observed that phospholipids coating the tubules were in a fluid liquid state.[25] Finally, the assembly happened at lower mole fraction of CholAU (<40 mol%) than the Chol saturation threshold (67 mol%) suggesting the important role for the uridine head group for the self-assembly of CholAU.

One other parameter that can be compared is the time needed for the needle structure assembly: cholesterol needles were formed within weeks, while CholAU needles were formed within hours to days. This is in line with the difference in the rate of micrometer sized tubules formation: cholesterol microtubules in bile salt were reported to form in about 3–6 days and were unstable;[6] CholAU–DOPC microtubules formed within minutes upon cooling from 70 °C to room temperature and were stable for months.[25]

We surmise that the differences in CholAU and Chol self-assembly might be due to the additional self-aggregating properties of the uridine head group of CholAU (stacking and hydrogen bonding) in comparison with just one hydrogen bond that could be formed by the OH group of Chol.

Conclusions

We have previously reported the self-assembly of CholAU with a phospholipid into nano- and microtubules containing about 80–90 mol% of CholAU starting from 30 : 70 CholAU : DOPC (molar ratio) multilamellar vesicles.[25] Incubation of the CholAU : DOPC mixture at 70 °C, presumably supporting the solubilization of CholAU in the DOPC membrane, and cooling to room temperature was reported to be essential for the formation of the tubular structures. Here we report that the nanotubules were formed even at room temperature when using solubilized CholAU and DMoPC giant unilamellar vesicles, indicating that the limiting factor is indeed the degree of incorporation of the conjugate into the lipid bilayer (the self-segregation and precipitation of CholAU). Different methods of CholAU addition were tested: incubation of pre-formed DMoPC : NBD-DMPC GUVs in flow chambers with 2.5 mM mβCD–CholAU; incubation of the GUVs in flow chambers with CholAU dissolved in DMSO; electroformation of GUVs from DMoPC : CholAU : NBD-DMPC mixtures in flow chambers;

addition of 2.5 mM mβCD–CholAU to DMoPC : NBD-DMPC GUVs in plastic tubes. The needle-like structures were formed in all samples when CholAU was present, although the rate of the formation strongly depended on the molar ratio of CholAU to total lipid in the sample. Moreover, we observed that the structures formed more promptly when CholAU was incorporated into the outer leaflet of the membrane, suggesting an intrinsic curvature effect due to the incorporation of the molecules. Transmission electron microscopy revealed that the needle-like structures represent tubules of 100–200 nm outer diameters and dense walls of 50–100 nm thickness. The inner lumen diameter of the tubules was in average 15–40 nm.

Our results reveal that nanometer sized tubules are intrinsic and stable structures formed in the binary system of cholesterylaminouridine and phosphatidylcholine even at room temperature. The novel assembly process described in this study opens the possibility to form such nanotubules in the presence of biological macromolecules for which high temperatures might be deleterious. Synthesis of cholesteryl nucleoside conjugates with other nucleobases for investigation of their ability to form nanotubules under similar conditions is presently underway in our laboratories.

Acknowledgements

References

1 G. M. Whitesides and B. Grzybowski, *Science*, 2002, **295**, 2418–2421.

2 J.-M. Lehn, *Proc. Natl. Acad. Sci. U. S. A.*, 2002, **99**, 4763–4768.

3 J. N. Israelachvili, D. J. Mitchell and B. W. Ninham, *J. Chem. Soc., Faraday Trans. 2*, 1976, **72**, 1525–1568.

4 P. R. Cullis and B. De Kruijff, *Biochim. Biophys. Acta*, 1979, **559**, 399–420.

5 A.-L. Fameau, F. Cousin, L. Navailles, F. Nallet, F. Boué and J.-P. Douliez, *J. Phys. Chem. B*, 2011, **115**, 9033–9039.

6 F. M. Konikoff, D. S. Chung, J. M. Donovan, D. M. Small and M. C. Carey, *J. Clin. Invest.*, 1992, **90**, 1155–1160.

7 G. S. Abela, *J. Clin. Lipidol.*, 2010, **4**, 156–164.

8 J. H. Jung, M. Park and S. Shinkai, *Chem. Soc. Rev.*, 2010, **39**, 4286–4302.

9 N. Kameta, H. Minamikawa and M. Masuda, *Soft Matter*, 2011, **7**, 4539–4561.

10 T. Shimizu, M. Masuda and H. Minamikawa, *Chem. Rev.*, 2005, **105**, 1401–1443.

11 A. Bot and W. G. M. Agterof, *JAOCS*, 2006, **83**, 513–521.

12 S. J. Lee, E. Kim, M. L. Seo, Y. Do, Y.-A. Lee, S. S. Lee, J. H. Jung, M. Kogiso and T. Shimizu, *Tetrahedron*, 2008, **64**, 1301–1308.

13 J. V. Trillo, F. Meijide, A. Jover, V. H. Soto, S. de Frutos, M. Chiara di Gregorio, L. Galantini and J. V. Tato, *RSC Adv.*, 2014, **4**, 5598–5606.

14 Z. Shen, T. Wang and M. Liu, *Chem. Commun.*, 2014, **50**, 2096–2099.

15 D. Berti, F. B. Bombelli, M. Fortini and P. Baglioni, *J. Phys. Chem. B*, 2007, **111**, 11734–11744.

16 C. Aimé, R. Tamoto, T. Satoh, A. Grelard, E. J. Dufourc, T. Buffeteau, H. Ihara and R. Oda, *Langmuir*, 2009, **25**, 8489–8496.

17 Y. V. Zastavker, N. Asherie, A. Lomakin, J. Pande, J. M. Donovan, J. M. Schnur and G. B. Benedek, *Proc. Natl. Acad. Sci. U. S. A.*, 1999, **96**, 7883–7887.

18 D. Q.-H. Wang, D. E. Cohen and M. C. Carey, *J. Lipid Res.*, 2009, S406–S411.

19 B. Jean, L. Oss-Ronen, P. Terech and Y. Talmon, *Adv. Mater.*, 2005, **17**, 728–731.

20 X. Zhang, J. Zou, K. Tamhane, F. F. Kobzeff and J. Fang, *Small*, 2010, **6**, 217–220.

21 V. H. Soto Tellini, A. Jover, F. Meijide, J. Vázquez Tato, L. Galantini and N. V. Pavel, *Adv. Mater.*, 2007, **19**, 1752–1756.

22 L. Galantini, C. Leggio, A. Jover, F. Meijide, N. V. Pavel, V. H. Soto Tellini, J. V. Tato, R. Di Leonardo and G. Ruocco, *Soft Matter*, 2009, **5**, 3018–3025.

23 E. Snip, K. Koumoto and S. Shinkai, *Tetrahedron*, 2002, **58**, 8863–8873.

24 Y. Jin, R. Xin, P. Ai and D. Chen, *Int. J. Pharm.*, 2008, **350**, 330–337.

25 P. Pescador, N. Brodersen, H. A. Scheidt, M. Loew, G. Holland, N. Bannert, J. Liebscher, A. Herrmann, D. Huster and A. Arbuzova, *Chem. Commun.*, 2010, **46**, 5358–5360.

26 O. Wesołowska, K. Michalak, J. Maniewska and A. B. Hendrich, *Acta Biochim. Pol.*, 2009, **56**, 33–39.

27 P. Walde, K. Cosentino, H. Engel and P. Stano, *ChemBioChem*, 2010, **11**, 848–865.

28 S. Chiantia, J. Ries and P. Schwille, *Biochim. Biophys. Acta*, 2009, **1788**, 225–233.

29 J. M. Holopainen, M. I. Angelova and P. K. Kinnunen, *Biophys. J.*, 2000, **78**, 830–838.

30 B. Sorre, A. Callan-Jones, J. Manzi, B. Goud, J. Prost, P. Bassereau and A. Roux, *Proc. Natl. Acad. Sci. U. S. A.*, 2012, **109**, 173–178.

31 M. Safouane, L. Berland, A. Callan-Jones, B. Sorre, W. Römer, L. Johannes, G. E. S. Toombes and P. Bassereau, *Traffic*, 2010, **11**, 1519–1529.

32 N. Kahya, D. Scherfeld, K. Bacia and P. Schwille, *J. Struct. Biol.*, 2004, **147**, 77–89.

33 N. Kahya, D. Scherfeld, K. Bacia, B. Poolman and P. Schwille, *J. Biol. Chem.*, 2003, **278**, 28109–28115.

34 D. Scherfeld, N. Kahya and P. Schwille, *Biophys. J.*, 2003, **85**, 3758–3768.

35 M. Loew, R. Springer, S. Scolari, F. Altenbrunn, O. Seitz, J. Liebscher, D. Huster, A. Herrmann and A. Arbuzova, *J. Am. Chem. Soc.*, 2010, **132**, 16066–16072.

36 M. Schade, A. Knoll, A. Vogel, O. Seitz, J. Liebscher, D. Huster, A. Herrmann and A. Arbuzova, *J. Am. Chem. Soc.*, 2012, **134**, 20490–20497.

37 T. Baumgart, G. Hunt, E. R. Farkas, W. W. Webb and G. W. Feigenson, *Biochim. Biophys. Acta*, 2007, **1768**, 2182–2194.

38 M. I. Angelova and D. S. Dimitrov, *Faraday Discuss.*, 1986, **81**, 303–311.

39 S. Chiantia, P. Schwille, A. S. Klymchenko and E. London, *Biophys. J.*, 2011, **100**, L01–L03.

40 H.-T. Cheng, Megha and E. London, *J. Biol. Chem.*, 2009, **284**, 6079–6092.

41 J. Yuan, S. M. Hira, G. F. Strouse and L. S. Hirst, *J. Am. Chem. Soc.*, 2008, **130**, 2067–2072.

42 M. H. Mohamed, L. D. Wilson, J. V Headley and K. M. Peru, *Rapid Commun. Mass Spectrom.*, 2009, **23**, 3703–3712.

43 C. A. López, A. H. de Vries and S. J. Marrink, *PLoS Comput. Biol.*, 2011, **7**, e1002020.

44 S. Milles, T. Meyer, H. A. Scheidt, R. Schwarzer, L. Thomas, M. Marek, L. Szente, R. Bittman, A. Herrmann, T. Günther Pomorski, D. Huster and P. Müller, *Biochim. Biophys. Acta*, 2013, **1828**, 1822–1828.

45 S. Grimmer, M. Ying, B. Van Deurs and K. Sandvig, *Traffic*, 2005, **6**, 144–156.

46 A.-F. Bitbol, N. Puff, Y. Sakuma, M. Imai, J.-B. Fournier and M. I. Angelova, *Soft Matter*, 2012, **8**, 6073–6082.

47 A. Papadopulos, S. Vehring, I. López-Montero, L. Kutschenko, M. Stöckl, P. F. Devaux, M. Kozlov, T. Pomorski and A. Herrmann, *J. Biol. Chem.*, 2007, **282**, 15559–15568.

48 U. Seifert, K. Berndl and R. Lipowsky, *Phys. Rev. A*, 1991, **44**, 1182–1202.

49 T. Tanaka, R. Sano, Y. Yamashita and M. Yamazaki, *Langmuir*, 2004, **20**, 9526–9534.

50 Y. Li, R. Lipowsky and R. Dimova, *Proc. Natl. Acad. Sci. U. S. A.*, 2011, **108**, 4731–4736.

51 R. Leventis and J. R. Silvius, *Biophys. J.*, 2001, **81**, 2257–2267.

52 K. John, J. Kubelt, P. Müller, D. Wüstner and A. Herrmann, *Biophys. J.*, 2002, **83**, 1525–1534.

53 R. Zidovetzki and I. Levitan, *Biochim. Biophys. Acta*, 2007, **1768**, 1311–1324.

54 Y. Yamashita, M. Oka, T. Tanaka and M. Yamazaki, *Biochim. Biophys. Acta*, 2002, **1561**, 129–134.

55 Y. Sun, C.-C. Lee, W.-C. Hung, F.-Y. Chen, M.-T. Lee and H. W. Huang, *Biophys. J.*, 2008, **95**, 2318–2324.

56 M. Yanagisawa, M. Imai and T. Taniguchi, *Phys. Rev. E*, 2010, **82**, 051928.

57 I. Visco, S. Chiantia and P. Schwille, *Langmuir*, 2014, **30**, 7475–7484.

58 I. Levental, M. Grzybek and K. Simons, *Proc. Natl. Acad. Sci. U. S. A.*, 2011, **108**, 11411–11416.

59 E. Baykal-Caglar, E. Hassan-Zadeh, B. Saremi and J. Huang, *Biochim. Biophys. Acta*, 2012, **1818**, 2598–2604.

60 J. Huang, J. T. Buboltz and G. W. Feigenson, *Biochim. Biophys. Acta*, 1999, **1417**, 89–100.

61 L. Mainali, M. Raguz and W. K. Subczynski, *J. Phys. Chem. B*, 2013, **117**, 8994–9003.

62 R. M. Epand, R. F. Epand, D. W. Hughes, B. G. Sayer, N. Borochov, D. Bach and E. Wachtel, *Chem. Phys. Lipids*, 2005, **135**, 39–53.

63 D. Marsh, *Biochim. Biophys. Acta*, 2010, **1798**, 688–699.

64 M. A. Barrett, S. Zheng, L. A. Toppozini, R. J. Alsop, H. Dies, A. Wang, N. Jago, M. Moore and M. C. Rheinstädter, *Soft Matter*, 2013, **9**, 9342–9351.

65 R. Ziblat, I. Fargion, L. Leiserowitz and L. Addadi, *Biophys. J.*, 2012, **103**, 255–264.

66 M. C. Frincu, S. D. Fleming, A. L. Rohl and J. A. Swift, *J. Am. Chem. Soc.*, 2004, **126**, 7915–7924.

67 P. Portincasa, A. Moschetta, K. J. van Erpecum, G. Calamita, A. Margari, G. P. VanBerge-Henegouwen and G. Palasciano, *Dig. Liver Dis.*, 2003, **35**, 118–126.

68 L. Hosta-Rigau, Y. Zhang, B. M. Teo, A. Postma and B. Städler, *Nanoscale*, 2013, **5**, 89–109.

69 J. Huang and G. W. Feigenson, *Biophys. J.*, 1999, **76**, 2142–2157.

70 R. Abendan and J. Swift, *Langmuir*, 2002, **11**, 4847–4853.

71 D. Q. Wang and M. C. Carey, *J. Lipid Res.*, 1996, **37**, 606–630.